Data Transmission by Frequency-Division Multiplexing Using the Discrete Fourier Transform

S. B. WEINSTEIN, MEMBER, IEEE, AND PAUL M. EBERT, MEMBER, IEEE

Abstract—**The Fourier transform data communication system is a realization of frequency-division multiplexing (FDM) in which discrete Fourier transforms are computed as part of the modulation and demodulation processes. In addition to eliminating the banks of subcarrier oscillators and coherent demodulators usually required in FDM systems, a completely digital implementation can be built around a special-purpose computer performing the fast Fourier transform. In this paper, the system is described and the effects of linear channel distortion are investigated. Signal design criteria and equalization algorithms are derived and explained. A differential phase modulation scheme is presented that obviates any equalization.**

I. Introduction

DATA ARE usually sent as a serial pulse train, but there has long been interest in frequency-division multiplexing with overlapping subchannels as a means of avoiding equalization, combating impulsive noise, and making fuller use of the available bandwidth. These "parallel data" systems, in which each member of a sequence of N digits modulates a subcarrier, have been studied in [2] and [4]. Multitone systems are widely used and have proved to be effective in [3], [8], and [9]. Fig. 1 compares the transmissions of a serial and a parallel system.

For a large number of channels, the arrays of sinusoidal generators and coherent demodulators required in parallel systems become unreasonably expensive and complex. However, it can be shown [1] that a multitone data signal is effectively the Fourier transform of the original serial data train, and that the bank of coherent demodulators is effectively an inverse Fourier transform generator. This point of view suggests a completely digital modem built around a special-purpose computer performing the fast Fourier transform (FFT). Fourier transform techniques, although not necessarily the signal format described in this paper, have been incorporated into several military data communication systems [5]–[7].

Because each subchannel covers only a small fraction of the original bandwidth, equalization is potentially simpler than for a serial system. In particular, for very narrow subchannels, soundings made at the centers of the subchannels may be used in simple transformations of the receiver output data to produce excellent estimates of the original data. Further, a simple equalization algorithm will minimize mean-square distortion on each subchannel, and differential encoding of the original data may make it possible to avoid equalization altogether.

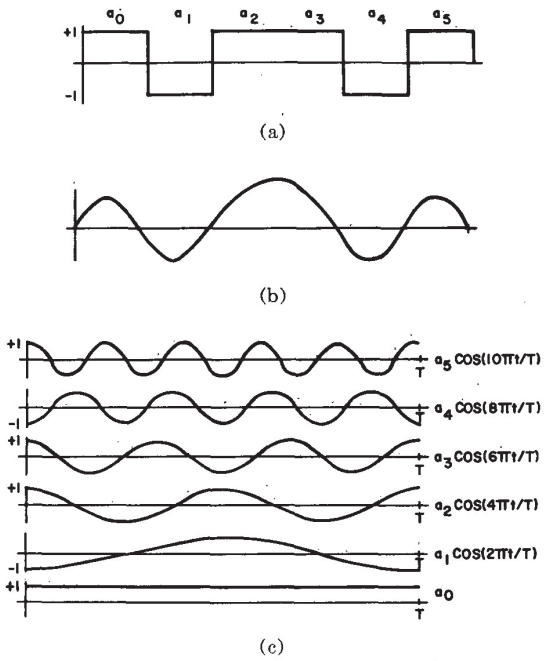


Fig. 1. Comparison of waveforms in serial and parallel data transmission systems. (a) Serial stream of six binary digits. (b) Typical appearance of baseband serial transmission. (c) Typical appearance of waveforms that are summed to create parallel data signals.

II. Frequency-Division Multiplexing as a Discrete Transformation

Consider a data sequence $(d_0, d_1, \cdots, d_{n-1})$, where each d_n is a complex number $d_n = a_n + jb_n$.

If a discrete Fourier transform (DFT) is performed on the vector $\{2d_n\}_{n=0}^{N-1}$, the result is a vector $S = (S_0, S_1, \cdots, S_{n-1})$ of N complex numbers, with

$$S_m = \sum_{n=0}^{N-1} 2d_n e^{-i(2\pi nm/N)} = 2\sum_{n=0}^{N-1} d_n e^{-i2\pi f_n t_m}$$
$$m = 0, 1, \cdots, N-1, \qquad (1)$$

where

$$f_n \triangleq \frac{n}{n\,\Delta t} \qquad (2)$$

Paper approved by the Data Communications Committee of the IEEE Communication Technology Group for publication after presentation at the 1971 IEEE International Conference on Communications, Montreal, Que., Canada, June 14–16. Manuscript received January 15, 1971; revised March 29, 1971.

The authors are with the Advanced Data Communications Department, Bell Telephone Laboratories, Holmdel, N. J.

Authorized licensed use limited to: Santa Clara University. Downloaded on August 10,2022 at 18:51:33 UTC from IEEE Xplore. Restrictions apply.

$$t_m \triangleq m\,\Delta t \tag{3}$$

and Δt is an arbitrarily chosen interval. The real part of the vector S has components

$$Y_m = 2\sum_{n=0}^{N-1}(a_n \cos 2\pi f_n t_m + b_n \sin 2\pi f_n t_m),$$
$$m = 0, 1, \cdots, N-1. \tag{4}$$

If these components are applied to a low-pass filter at time intervals Δt, a signal is obtained that closely approximates the frequency-division multiplexed signal

$$y(t) = 2\sum_{n=0}^{N-1}(a_n \cos 2\pi f_n t + b_n \sin 2\pi f_n t),$$
$$0 \le t \le N\,\Delta t. \tag{5}$$

A block diagram of the communication system in which $y(t)$ is the transmitted signal appears in Fig. 2.

Demodulation at the receiver is carried out via a discrete Fourier transformation of a vector of samples of the received signal. Because only the real part of the Fourier transform has been transmitted, it is necessary to sample twice as fast as expected, i.e., at intervals $\Delta t/2$. When there is no channel distortion, the receiver DFT operates on the $2N$ samples

$$Y_k = y\left(k\frac{\Delta t}{2}\right) = 2\sum_{n=0}^{N-1}\left(a_n \cos\frac{2\pi nk}{2N} + b_n \sin\frac{2\pi nk}{2N}\right),$$
$$K = 0, 1, \cdots, 2N-1, \tag{6}$$

where definitions (2) and (3) have been substituted into (4). The DFT yields

$$z_l = \frac{1}{2N}\sum_{k=0}^{2N-1} Y_k e^{-j(2\pi lk/2N)} = \begin{cases} 2a_0, & l = 0 \\ a_l - jb_l, & l = 1, 2, \cdots, N-1 \\ \text{irrelevant}, & l > N-1, \end{cases} \tag{7}$$

where the equality

$$\frac{1}{2N}\sum_{k=0}^{2N-1} e^{j(2\pi mk/2N)} = \begin{cases} 1, & m = 0, \pm 2N, \pm 4N, \cdots \\ 0, & \text{otherwise} \end{cases} \tag{8}$$

has been employed. The original data a_l and b_l are available (except for $l = 0$) as the real and imaginary components, respectively, of z_l, as indicated in Fig. 2. A synchronizing signal is required, but one or several channels of the transmitted signal can readily be utilized for this purpose.

Because the sinusoidal components of the parallel data signal $y(t)$ are truncated in time, the power density spectrum of $y(t)$ consists of $[\sin(f)/f]^2$-shaped spectra, as sketched in Fig. 3. Nevertheless, the data on the different subchannels can be completely separated by the DFT operation of (7). This will not be exactly true when linear channel distortion affects the received signal, but it will be shown later that a modest reduction in transmission rate eliminates most interferences.

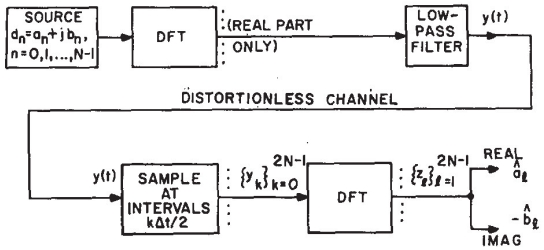


Fig. 2. Fourier transform communication system in absence of channel distortion.

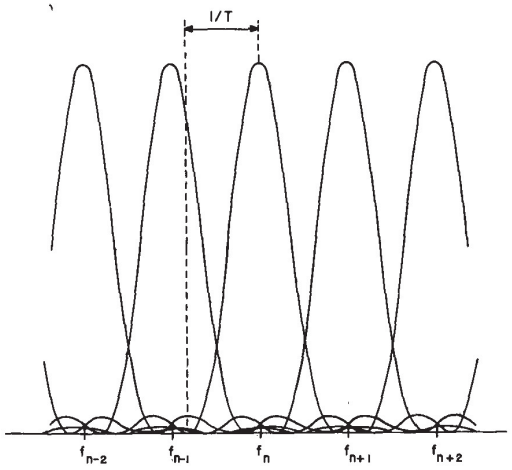


Fig. 3. Power density spectra of subchannel components of $y(t)$.

III. Equalization by Use of Channel Soundings

Except for the added linear channel distortion and final equalizer, the Fourier transform data communication system shown in Fig. 4 is identical to that of Fig. 2. Ideally, the discrete Fourier transformation in the receiver should be replaced by another linear transformation, derived in [1], which minimizes the error in the receiver output. However, it is preferable, if possible, to retain the DFT with its "fast" implementations and carry out suboptimal but adequate correctional transformations at the receiver output. The system of Fig. 4 performs this approximate equalization.

Consider the waveform at the receiver input,

$$r(t) = y(t) * h(t), \tag{9}$$

where the asterisk denotes convolution. This waveform is a collection of truncated sinusoids modified by a linear filter. If the sinusoid $\cos 2\pi f_n t$ were not truncated, then the result of passing it through a channel with transfer function $H(f)$ would be $H_n \cos(2\pi f_n t + \phi_n)$, where

$$H_n = |H(f_n)| \qquad \phi_n = \tan^{-1}\left(\frac{\text{Im } H(f_n)}{\text{Re } H(f_n)}\right). \tag{10}$$

The sinusoids in the transmitted signal $y(t)$ [see (5)] are truncated to the interval $(0, N\Delta t)$, so that the nth subchannel must accommodate a $[\sin N\pi(f - f_n)\Delta t]/$

Authorized licensed use limited to: Santa Clara University. Downloaded on August 10,2022 at 18:51:33 UTC from IEEE Xplore. Restrictions apply.

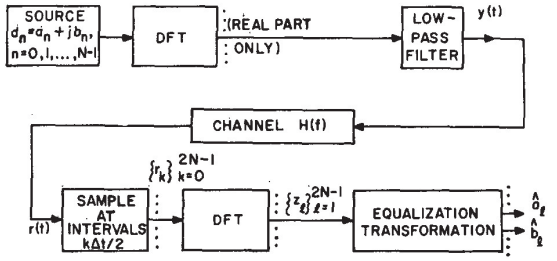


Fig. 4. Fourier transform communication system including linear channel distortion and final equalization.

$[N\pi(f - f_n)\Delta t]$ spectrum instead of the impulse at f_n, which would correspond to a pure sinusoid. However, if $1/(N\Delta t)$ is small compared with the total transmission bandwidth, then $H(f)$ does not change significantly over the subchannel and an approximate expression for the received signal $r(t)$ is

$$\begin{aligned} r(t) &\cong 2\sum_{n=1}^{N-1} H_n[a_n \cos(2\pi f_n t + \phi_n) \\ &\qquad + b_n \sin(2\pi f_n t + \phi_n)] + 2H_0 a_0 \\ &= 2\sum_{n=1}^{N-1} H_n[(a_n \cos\phi_n + b_n \sin\phi_n)\cos 2\pi f_n t \\ &\qquad + (b_n \cos\phi_n - a_n \sin\phi_n)\sin 2\pi f_n t] \\ &\qquad + 2H_0 a_0, \qquad 0 \le t \le N\,\Delta t. \end{aligned} \tag{11}$$

As indicated in Fig. 4, $r(t)$ is sampled at times $k(\Delta t/2)$, $k = 0, 1, \cdots, 2N-1$, and the samples $\{r_k\}$ are applied to a discrete Fourier transformer. The output of the DFT is

$$\begin{aligned} z_l &= \frac{1}{2N}\sum_{k=0}^{2N-1} r_k e^{-j(2\pi lk/2N)} \\ &\cong \begin{cases} 2H_0 a_0, & l = 0 \\ H_l[a_l \cos\phi_l + b_l \sin\phi_l] - H_l[b_l \cos\phi_l \\ \quad - a_l \sin\phi_l], & l = 1, 2, \cdots, N-1 \\ \text{irrelevant}, & l > N-1. \end{cases} \end{aligned} \tag{12}$$

Estimates of a_l and b_l are obtained from the computations

$$\left.\begin{aligned} \hat{a}_l &= \frac{1}{H_l}[\mathrm{Re}\,(z_l)\cos\phi_l + \mathrm{Im}\,(z_l)\sin\phi_l] \\ \hat{b}_l &= \frac{1}{H_l}[\mathrm{Re}\,(z_l)\sin\phi_l - \mathrm{Im}\,(z_l)\cos\phi_l] \end{aligned}\right\}, \qquad l = 1, 2, \cdots, N-1. \tag{13a}$$

In complex notation, the appropriate computation is

$$\hat{a}_l - j\hat{b}_l = w_l z_l, \tag{13b}$$

where

$$w_l = \frac{1}{H_l}[\cos\phi_l - j\sin\phi_l]. \tag{13c}$$

Equations (13a–c) describe a 2×2 transformation to be performed on each of the DFT outputs z_l, $l = 1, 2, \cdots, N-1$. For a reasonably large N and a typical communication channel, the approximation of $H(f)$ by a constant over each subchannel, which leads to (13a–c), may be adequate. However, linear rather than constant approximations to the amplitude and phase of the channel transfer function as it affects each subchannel waveform are much closer to reality. The following section examines the consequences of these approximations. It is shown that the truncated subchannel sinusoids are delayed by differing amounts, and that distortion is concentrated at the on–off transitions of these waveforms. Further, the magnitude of the distortion is proportional to the abruptness of the transitions. Hence a "guard space," consisting of a modest increase in the signal duration together with a smoothing of the on–off transitions, will eliminate most interference among channels and between adjacent transmission blocks. The individual channels can then be equalized in accord with (13a–c).

IV. Approximate Analysis of the Effects of Channel Distortion

The transmitted signal $y(t)$ as given by (5) exists only on the interval $(0, N\Delta t)$, so that each subchannel must, as noted earlier, accommodate a $\sin f/f$ type spectrum. As suggested in the last section, let this spectrum be narrowed by increasing the signal duration to some $T > N\,\Delta\,t$ and requiring gradual rather than abrupt rolloffs of the transmitted waveform. Specifically, the transmitted signal will be redefined as

$$y(t) = 2g_a(t)\sum_{n=0}^{N-1}[a_n \cos(2\pi f_n t) + b_n \sin(2\pi f_n t)], \tag{14}$$

where an appropriate $g_a(t)$ is

$$g_a(t) = \begin{cases} \frac{1}{2}\left[1 + \cos\frac{\pi t}{2aT}\right], & -2aT \le t < 0 \\ 1, & 0 \le t < T \\ \frac{1}{2}\left[1 + \cos\frac{\pi(t-T)}{2aT}\right], & T \le t < (1+2a)T \\ 0 \quad \text{elsewhere.} \end{cases} \tag{15}$$

The "window function" $g_a(t)$ is sketched in Fig. 5.

When $y(t)$ is passed through the channel filter with impulse response $h(t)$, the received signal is

$$\begin{aligned} r(t) &= \sum_{n=0}^{N-1}\{a_n[2h(t)*g_a(t)\cos 2\pi f_n t] \\ &\qquad + b_n[2h(t)*g_a(t)\sin 2\pi f_n t]\} \\ &= \sum_{n=0}^{N-1}\{a_n q_a^{(n)}(t) + b_n q_b^{(n)}(t)\}, \end{aligned} \tag{16}$$

Authorized licensed use limited to: Santa Clara University. Downloaded on August 10,2022 at 18:51:33 UTC from IEEE Xplore. Restrictions apply.



Fig. 5. Window $g_a(t)$ multiplying all subchannel sinusoids in transmitted signal.

where

$$q_a^{(n)}(t) = 2h(t) * g_a(t) \cos 2\pi f_n t$$
$$q_b^{(n)}(t) = 2h(t) * g_a(t) \sin 2\pi f_n t. \quad (17)$$

In Appendix I, linear approximations to the amplitude and phase of $H(f)$ around $f = \pm f_n$ result in the following approximate expression for $q_a^{(n)}(t)$.

$$q_a^{(n)}(t) \cong 2H_n \cos [2\pi f_n t + \phi_n] g_a(t - \beta_n) + \frac{\alpha_n}{\pi} \sin [2\pi f_n t + \phi_n] \frac{d}{dt} g_a(t - \beta_n), \quad (18)$$

where (H_n, ϕ_n) is the channel sounding at frequency f_n, and α_n and β_n are the slopes at $f = f_n$ of the linear approximations to amplitude and phase of $H(f)$, as shown in Fig. 6. A similar expression results for $q_b^{(n)}(t)$. The first term on the right-hand side of (18) is the nth cosine element in the transmitted signal (14), except that it is modified by a channel sounding (H_n, ϕ_n) and subjected to an envelope delay β_n. Interblock interference can result if a delayed sinusoid from a previous block impinges on the current sampling period. The second term is distortion arising from the amplitude variations of $H(f)$, and it is a potential source of interchannel interference. Suppose, however, that T is large enough so that

$$T > (2N - 1) \frac{\Delta t}{2} + \max_n (\beta_n) - \min_n (\beta_n), \quad (19)$$

as pictured in Fig. 7. Then for all n there exists a time $t_0 > \max \beta_n$ such that

$$\frac{d}{dt} g_a(t - \beta_n) = 0, \qquad t_0 \leq t \leq (2N - 1) \frac{\Delta t}{2} + t_0. \quad (20)$$

Fig. 7 shows where the interval $(t_0, t_0 + (2N - 1)(\Delta t/2))$ is located with respect to the minimum and maximum values of the time shift β_n. Thus,

$$q_a^{(n)}(t) \cong 2H_n \cos (2\pi f_n t + \phi_n), \qquad t_0 \leq t \leq t_0 + \frac{(2N - 1)\,\Delta t}{2}. \quad (21)$$

By a similar derivation,

$$q_b^{(n)}(t) \cong 2H_n \sin (2\pi f_n t + \phi_n), \qquad t_0 \leq t \leq t_0 + \frac{(2N - 1)\,\Delta t}{2}. \quad (22)$$

Therefore, substituting (21) and (22) into (16) (except for $n = 0$),

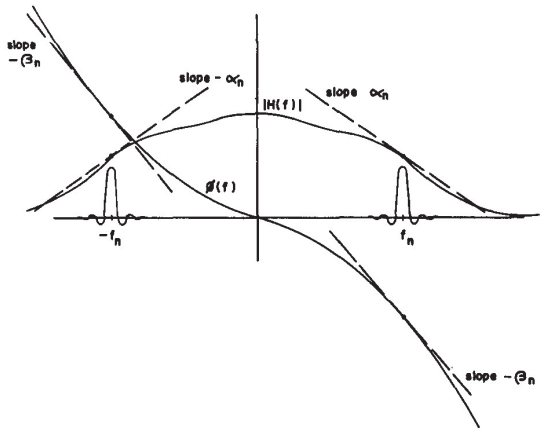


Fig. 6. Linear approximations to amplitude and phase of $H(f)$ in relation to spectra $G_a(f - fn)$ and $G_a(f + fn)$.

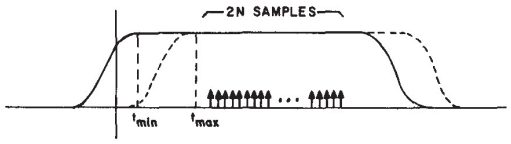


Fig. 7. Shifted versions of $g_a(t)$ corresponding to subchannels with minimum and maximum delay and locations of samples taken by receiver. Here $t_{min} = \min_n \beta_n$, $t_{max} = \max_n \beta_n$.

$$r(t) \cong 2 \sum_{n=1}^{N-1} H_n [a_n \cos (2\pi f_n t + \phi_n) + b_n \sin (2\pi f_n t + \phi_n)] + 2H_0 a_0, \qquad t_0 \leq t \leq t_0 + (2N - 1) \frac{\Delta t}{2}. \quad (23)$$

Except for the shifted domain of definition, (23) is identical to (11), which led to (13) for retrieval of the data. It can be shown that initiating sampling of $r(t)$ at $t = t_0$ instead of at $t = 0$ is equivalent to incrementing each phase ϕ_l by $f_l\, t_0$ rad in the equalization equations (13).

Intuitively, $r(t)$ reduces to (23) because linear distortion delays different spectral components by different amounts and responds to abrupt transitions with "ringing." If the subchannel waveforms are examined during an interval when they are all present, and if all the on–off transitions lie well outside this interval, then the waveforms will look like the collection of sinusoids described by (5). The linear approximations to amplitude and phase of $H(f)$ restrict the ringing from the transition periods to those periods themselves. In practice, the ringing can be expected to die out very rapidly outside of the transition periods. This use of a guard space is a common technique, as, for example, described in [3].

V. Algorithm for Minimizing Mean-Square Distortion

Under the assumption supported by the results of the last section that interchannel interference is negligible, a simple algorithm can be devised for determination of the

Authorized licensed use limited to: Santa Clara University. Downloaded on August 10,2022 at 18:51:33 UTC from IEEE Xplore. Restrictions apply.

parameters $\cos \phi_l/H_l$ and $\sin \phi_l/H_l$ on each channel, which minimize mean-square distortion when used in the transformation of (13a–c). Because of propagation delay and the presence of noise, these parameters may not exactly correspond to a sounding of the lth subcarrier channel. The use of an automatic equalization procedure based on the minimum mean-square distortion algorithm leads to accurate demodulation without having to make precise channel soundings. Further, the algorithm can work adaptively after an initial coarse adjustment.

The receiver produces estimates $\hat{a}_l$ and $\hat{b}_l$ according to the formulas

$$\begin{aligned} \hat{a}_l &= T_{1l} \operatorname{Re} Z_l + T_{2l} \operatorname{Im} Z_l \\ \hat{b}_l &= T_{2l} \operatorname{Re} Z_l - T_{1l} \operatorname{Im} Z_l, \end{aligned} \tag{24}$$

which resemble (13a–c), except that the T coefficients are to be chosen to minimize the estimation error.[1] Mean-square distortion is defined by

$$\begin{aligned} \epsilon &= E \sum_{l=1}^{N-1} [e_{la}^2 + e_{lb}^2] \\ &= E \sum_{l=1}^{N-1} [(T_{1l} \cdot \operatorname{Re} Z_l + T_{2l} \cdot \operatorname{Im} Z_l - a_l)^2 \\ &\qquad + (T_{2l} \cdot \operatorname{Re} Z_l - T_{1l} \cdot \operatorname{Im} Z_l - b_l)^2], \end{aligned} \tag{25}$$

where

$$\begin{aligned} e_{la} &\triangleq \hat{a}_l - a_l \\ e_{lb} &\triangleq \hat{b}_l - b_l. \end{aligned} \tag{26}$$

It is shown in Appendix II that ϵ is a convex function of the vector $\bar{T}$, where

$$\bar{T} = (T_{11}, T_{21}, T_{12}, T_{22}, \cdots, T_{1(n-1)}, T_{2(n-1)}). \tag{27}$$

Thus a steepest descent algorithm is sure to converge to the vector $\bar{T}_0$ yielding the minimum mean-square distortion.

The $l_{1,2}$th components of the gradient of ϵ with respect to $\bar{T}$ are

$$\begin{aligned} (\nabla\epsilon)_{l1} &= \frac{\partial \epsilon}{\partial T_{1l}} = E[2e_{la} \operatorname{Re} Z_l - 2e_{lb} \operatorname{Im} Z_l] \\ (\nabla\epsilon)_{l2} &= \frac{\partial \epsilon}{\partial T_{2l}} = E[2e_{la} \operatorname{Im} Z_l + 2e_{lb} \operatorname{Re} Z_l]. \end{aligned} \tag{28}$$

The steepest descent algorithm makes changes at the end of each block transmission in a direction opposite to the gradient:

$$\begin{aligned} \Delta T_{1l} &= -k[e_{la} \operatorname{Re} Z_l - e_{lb} \operatorname{Im} Z_l] \\ \Delta T_{2l} &= -k[e_{la} \operatorname{Im} Z_l + e_{lb} \operatorname{Re} Z_l], \end{aligned} \tag{29}$$

where k controls the step size. A block diagram of the implementation of (30) is shown in Fig. 8. The initial value of $\bar{T}$ is probably best obtained from crude channel soundings, or specified as some "typical" vector quantity. It is expected that the first round of adjustments, made at the end of the first block transmission, will suffice to reduce the error to a low level, if it is not already low with the initial value of $\bar{T}$. At $\Delta t = 0.5$ ms, the length of one block before addition of a guard space will vary from about 8 ms (16 subchannels) to about 64 ms (128 subchannels). This block length, plus the guard space necessary to minimize interference, is a transmission delay that cannot be avoided.

The equalization algorithm given here only equalizes distortion due to cochannel interference (channels on the same frequency) and completely ignores interchannel interference. An unpublished analysis by the authors shows that for this equalizer, the interchannel interference becomes arbitrarily small as the number of subchannels increases. This is true even without any of the signal modification described in Section IV.

VI. Transmission Without Equalization

We have shown that for narrow subchannels the channel can be equalized by multiplying z_l, the receiver output for the lth subcarrier channel, by a number w_l [see (13c)]. This is simply compensation for attenuation and phase shift in that particular subchannel. The interference among subchannels is made small by using a guard time and smooth transitions between blocks.

For binary transmission, the attenuation need not be compensated, and if differential phase transmission between subchannels is used, no phase equalization is needed. In order for this technique to work, the difference in phase of the transmission channel transfer function $H(f)$ between adjacent subchannels should be small. Assume this is the case and let

$$d_n = (a_n - jb_n)d_{n-1}, \tag{30}$$

where a_n and b_n are binary information digits on the nth subchannel. For the first block transmission, d_0 is necessarily a fixed reference. At the output of the DFT in the receiver, form the product

$$\begin{aligned} z_n z_{n-1}^* &= h_n d_n h_{n-1}^* d_{n-1}^* \\ &= (a_n - jb_n) |h_n|^2 |d_{n-1}|^2 \\ &\quad + (a_n - jb_n) h_n (h_{n-1}^* - h_n^*) |d_{n-1}|^2, \\ &\qquad n = 1, 2, \cdots, N-1, \end{aligned} \tag{31}$$

where $h_n = H(f_n)$ is the complex channel transfer function at the center frequency of the nth subchannel. The last part of (31) is the information signal times an unknown amplitude term, plus an error term depending on $h_n - h_{n-1}$. For binary transmission, the information signal can be reliably recovered if the second term is less than half of the first term. This is equivalent to saying that the phase of h does not change by more than

[1] The vector $\bar{T}$ and its subscripted components should not be confused with the signal duration T used earlier.

Authorized licensed use limited to: Santa Clara University. Downloaded on August 10,2022 at 18:51:33 UTC from IEEE Xplore. Restrictions apply.

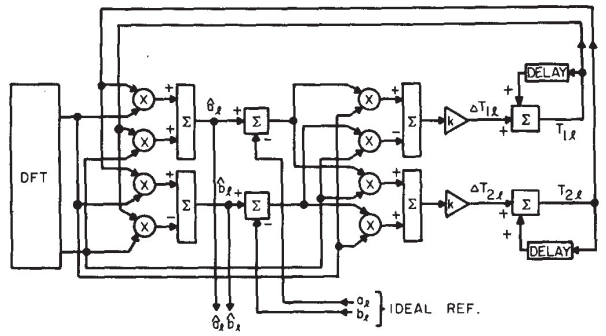


Fig. 8. Automatic equalizer for Fourier transform receiver. One such apparatus is required for each of the $(n-1)$ usable outputs of the discrete Fourier transformer.

30° between the centers of adjacent subchannels. Because a_n and b_n are binary, $(a_n - jb_n)$ may be recovered by determining which quadrant of the complex plane contains $z_n z_{n-1}^*$, even though h_n is unknown.

For the second and all subsequent block transmissions, d_0 can carry information by comparing it with d_0 from the previous T-second transmission, i.e.,

$$d_{0\ \text{current}} = (a_0 - jb_0)d_{0\ \text{previous}}. \tag{32}$$

Appendix I

Received Signal Under Linear Approximations to Amplitude and Phase of the Channel Transfer Function

The received signal is given by (16) as

$$r(t) = \sum_{n=0}^{N-1} [a_n q_a^{(n)}(t) + b_n q_b^{(n)}(t)], \tag{33}$$

where

$$\begin{aligned} q_a^{(n)}(t) &= 2h(t) * [g_a(t) \cos (2\pi f_n t)] \\ q_b^{(n)}(t) &= 2h(t) * [g_a(t) \sin (2\pi f_n t)]. \end{aligned} \tag{34}$$

Restricting attention for the time being to $q_a^{(n)}(t)$, the Fourier transform of this function is

$$Q_a^{(n)}(f) = H(f)[G_a(f - f_n) + G_a(f + f_n)], \tag{35}$$

where $G_a(f)$ is the Fourier transform of the "window function" $g_a(t)$. We now make linear approximations to the amplitude and phase of $H(f)$ as they affect the separate spectra $G_a(f - f_n)$ and $G(f + f_n)$ in (35). For $G_a(f - f_n)$, the approximation is

$$H(f) \cong [H_n + \alpha_n(f - f_n)]e^{j[\phi_n - \beta_n(f - f_n)]}, \tag{36}$$

and for $G_a(f + f_n)$ the approximation is

$$H(f) \cong [H_n - \alpha_n(f - f_n)]e^{-j[\phi_n + \beta_n(f + f_n)]}. \tag{37}$$

The validity of these approximations depends on the narrowness of $G_a(f)$ and the size of f_n, as illustrated in Fig. 6. One can always select a window function $g_a(t)$ for which the approximations of (36) and (37) lead to arbitrarily accurate expressions for $q_a^{(n)}(t)$ and $q_b^{(n)}(t)$ except for the lowest values of n.

Substituting approximations (36) and (37) into (35),

$$\begin{aligned} Q_a^{(n)}(f) \cong\ & [H_n + \alpha_n(f - f_n)]e^{j[\phi_n - \beta_n(f - f_n)]} \\ & + [H_n - \alpha_n(f - f_n)]e^{-j[\phi_n + \beta_n(f + f_n)]}G_a(f + f_n). \end{aligned} \tag{38}$$

Thus

$$\begin{aligned} q_a^{(n)}(t) &= \int_{-\infty}^{\infty} Q_a^{(n)}(f)e^{j2\pi ft}\, df \\ &\cong \int_{-\infty}^{\infty} [H_n + \alpha_n(f - f_n)]e^{j[\phi_n - \beta_n(f - f_n)]} \\ &\quad \cdot G_a(f - f_n)e^{j2\pi ft}\, df + \int_{-\infty}^{\infty} [H_n - \alpha_n(f + f_n)] \\ &\quad \cdot e^{-j[\phi_n + \beta_n(f + f_n)]}G_a(f + f_n)e^{j2\pi ft}\, df. \end{aligned} \tag{39}$$

After appropriate changes of variable, these Fourier transforms can be evaluated by recalling the following Fourier transform pairs

$$\begin{aligned} x(t - t_0) &\Leftrightarrow e^{-jft_0}X(f) \\ \frac{d}{dt}x(t - t_0) &\Leftrightarrow j2\pi fe^{-jft_0}X(f). \end{aligned} \tag{40}$$

Thus

$$\begin{aligned} q_a^{(n)}(t) \cong\ & 2H_n \cos [2\pi f_n t + \phi_n]g_a(t - \beta_n) \\ & + \frac{\alpha_n}{\pi} \sin [2\pi f_n t + \phi_n] \frac{d}{dt} g_a(t - \beta_n). \end{aligned} \tag{41}$$

This approximation appears as (19) in the main body of this paper. A similar derivation yields an analogous approximation to $q_b^{(n)}(t)$.

Appendix II

Convexity of Mean-Square Error

The mean-square error has been defined as

$$\begin{aligned} \epsilon(\bar{T}) = E \sum_{l=1}^{N-1} \{ & [T_{1l} \operatorname{Re} z_l + T_{2l} \operatorname{Im} z_l - a_l]^2 \\ & + [T_{2l} \operatorname{Re} z_l - T_{1l} \operatorname{Im} z_l - b_l]^2 \}, \end{aligned} \tag{42}$$

where the vector $\bar{T}$ is defined as

$$\bar{T} = (T_{11}, T_{21}, T_{22}, T_{22}, \cdots, T_{1(N-1)}, T_{2(N-1)}). \tag{43}$$

Taking a single term of the sum, we have

$$\begin{aligned} & T_{1l}^2(\operatorname{Re} z_l)^2 + T_{2l}^2(\operatorname{Im} z_l)^2 + 2 \operatorname{Re} Z_l \operatorname{Im} z_l T_{1l} T_{2l} \\ & \quad - 2a_l[T_{1l} \operatorname{Re} z_l + T_{2l} \operatorname{Im} z_l] + a_l^2 + T_{2l}^2(\operatorname{Re} z_l)^2 \\ & \quad + T_{2l}^2(\operatorname{Im} z_l)^2 - 2 \operatorname{Re} z_l \operatorname{Im} z_l T_{1l} T_{2l} \\ & \quad - 2b_l[T_{2l} \operatorname{Re} z_l - T_{1l} \operatorname{Im} z_l] + b_l^2 \\ & = (T_{1l}^2 + T_{2l}^2)\, |z_l|^2 + 2T_{1l}(b_l \operatorname{Im} z_l - a_l \operatorname{Re} z_l) \\ & \quad - 2T_{2l}(a_l \operatorname{Im} z_l + b_l \operatorname{Re} z_l) + a_l^2 + b_l^2, \end{aligned}$$

Authorized licensed use limited to: Santa Clara University. Downloaded on August 10,2022 at 18:51:33 UTC from IEEE Xplore. Restrictions apply.

which is the sum of convex functions and is thus convex itself. Since $\epsilon(\bar{T})$ is the sum of convex functions, it too is convex.

ACKNOWLEDGMENT

The authors are indebted to J. E. Mazo for comments on approximation techniques, and to J. Salz for earlier work on this project.

REFERENCES

[1] J. Salz and S. B. Weinstein, "Fourier transform communication system," presented at the Ass. Comput. Machinery Conf. Computers and Communication, Pine Mountain, Ga., Oct. 1969.
[2] B. R. Salzberg, "Performance of an efficient parallel data transmission system," *IEEE Trans. Commun. Technol.*, vol. COM-15, Dec. 1967, pp. 805–811.
[3] M. L. Doelz, E. T. Heald, and D. L. Martin, "Binary data transmission techniques for linear systems," *Proc. IRE*, vol. 45, May 1957, pp. 656–661.
[4] R. W. Chang and R. A. Gibby, "A theoretical study of performance of an orthogonal multiplexing data transmission scheme," *IEEE Trans. Commun. Technol.*, vol. COM-16, Aug. 1968, pp. 529–540.
[5] E. N. Powers and M. S. Zimmerman, "TADIM—A digital implementation of a multichannel data modem," presented at the 1968 IEEE Int. Conf. Communications, Philadelphia, Pa.
[6] W. W. Abbott, R. C. Benoit, Jr., and R. A. Northrup, "An all-digital adaptive data modem," presented at the IEEE Computers and Communication Conf., Rome, N. Y., 1969.
[7] W. W. Abbott, L. W. Blocker, and G. A. Bailey, "Adaptive data modem," Page Commun. Eng., Inc., RADC—TR-69-296, Sept. 1969.
[8] M. S. Zimmerman and A. L. Kirsch, "The AN/GSC-10 (KATHRYN) variable rate data modem for HF radio," *IEEE Trans. Commun. Technol.*, vol. COM-15, Apr. 1967, pp. 197–204.
[9] J. L. Holsinger, "Digital communication over fixed time-continuous channels with memory, with special applications to telephone channels," M.I.T. Res. Lab. Electron., Cambridge, Rep. 430, 1964.



S. B. Weinstein (S'59–M'66) was born in New York, N. Y., on November 25, 1938. He received the B.S. degree from the Massachusetts Institute of Technology, Cambridge, in 1960, the M.S. degree from the University of Michigan, Ann Arbor, in 1962, and the Ph.D. degree from the University of California, Berkeley, in 1966.

Upon finishing his graduate studies he worked for approximately one year with the Philips Research Laboratories in Eindhoven, the Netherlands, before joining the Advanced Data Communications Department at Bell Telephone Laboratories, Holmdel, N. J., in 1968. He works in the areas of statistical communication theory and data communications.



Paul M. Ebert (M'60) was born in Madison, Wis., on December 30, 1935. He received the B.S. degree from the University of Wisconsin, Madison, in 1958, and the M.S. and Sc D. degrees from the Massachusetts Institute of Technology, Cambridge, in 1962 and 1965, respectively.

From 1958 to 1960 he was a member of the Airborne Communications Division at the Radio Corporation of America, Camden, N. J. Since 1965 he has been a member of the Advanced Data Communications Department, Bell Telephone Laboratories, Holmdel, N. J. He has worked in the fields of information theory, coding, and digital filtering.

Eye Pattern for the Binary Noncoherent Receiver

see Section C

WILLIAM F. McGEE, MEMBER, IEEE

Abstract—**The assessment of imperfect channels in data transmission usually involves noise considerations. Channel imperfections are related to system performance by determining the increase in carrier-to-noise ratio required to maintain a fixed error rate. The impairment is determined by examining the "eye" pattern, which shows the effective reduction in signal amplitude caused by intersymbol interference.**

This paper derives the eye function for the binary quadratic receiver. The binary instantaneous frequency discriminator, the differential phase shift receiver, and the noncoherent frequency-shift keying (FSK) receiver implemented using the difference of two envelopes are binary quadratic receivers.

The eye pattern is easily obtained by computation using the eye function.

Paper approved by the Data Communications Committee of the IEEE Communication Technology Group for publication after presentation at the 1970 IEEE International Conference on Communications, San Francisco, Calif., June 8–10. Manuscript received September 22, 1970.

The author is with Bell-Northern Research, Ottawa, Ont., Canada.

I. INTRODUCTION

A USEFUL design method for determining the effect of channel distortions on a linearly modulated and demodulated signal is to use the eye-opening criterion, which basically determines the distance from the decision threshold for the worst data sequence. This distance allows the designer to determine the increase in carrier power necessary to correct for this distortion.

With the noncoherent quadratic receiver it is difficult to perform a comparable analysis. Thus, in the preliminary treatment of such systems it is common to assume that the noise power is that obtained through a filter with a bandwidth equal to the signaling speed, whereas the signal is undistorted. It is then necessary to determine the increase in carrier-to-noise (C/N) ratio that would be necessary with the actual channel. To

Authorized licensed use limited to: Santa Clara University. Downloaded on August 10,2022 at 18:51:33 UTC from IEEE Xplore. Restrictions apply.